International Journal of Radiology Sciences

ISSN Print: 2664-9810
ISSN Online: 2664-9829
IJRC 2025; 7(2): 23-28
www.radiologyjournals.com
Received: 11-05-2025
Accepted: 16-06-2025

Haydar Abdulkadeer Taheer Al-Shimmari
1. Department of Radiological Techniques, College of Health and Medical Techniques/Baghdad, Middle Technical University, 10047BabAlMuadham, Baghdad, Iraq,
2. Department of Radiology and Imaging, Faculty of Medicine and Health Sciences, University Putra Malaysia, 43400 Serdang, Selangor, Malaysia

Corresponding Author:
Haydar Abdulkadeer Taheer Al-Shimmari
1. Department of Radiological Techniques, College of Health and Medical Techniques/Baghdad, Middle Technical University, 10047BabAlMuadham, Baghdad, Iraq,
2. Department of Radiology and Imaging, Faculty of Medicine and Health Sciences, University Putra Malaysia, 43400 Serdang, Selangor, Malaysia

Improving glioblastoma delineation through TR and flip angle optimization in post-contrast T_1-weighted MRI at 1.5 tesla

Haydar Abdulkadeer Taheer Al-Shimmari

DOI: https://www.doi.org/10.33545/26649810.2025.v7.i2a.38

Abstract
Background: Accurate glioblastoma imaging after contrast administration is vital for surgical planning, radiotherapy targeting, and monitoring. Comparative evidence on protocol performance and parameter optimization at 1.5 Tesla remains limited.
Purpose: To compare two post-contrast T_1-weighted MRI protocols—GEM-LT (gradient-echo-based) and TESIP (spin-echo-based)—and evaluate the impact of repetition time (TR) and flip angle (FA) refinement on lesion conspicuity.
Methods: Fifty patients with histopathologically confirmed glioblastoma underwent 1.5T MRI using GEM-LT and TESIP protocols. TESIP was tested in standard form (TR = 500 ms, FA = 90°) and modified form (TR = 700 ms, FA = 110°). Signal intensity (SI) was measured from 30 ROIs per patient, targeting the enhancing tumor core, peritumoral edema, and contralateral white matter. Statistical comparisons used one-way ANOVA with LSD post-hoc tests; effect sizes were reported.
Results: TESIP produced higher mean SI than GEM-LT (2082.97 ± 128.05 vs. 1931.83 ± 126.75; $p < 0.001$; $\eta^2 = 0.264$). Parameter refinement in TESIP further increased SI (2187.12 ± 130.45; $p < 0.001$; $\eta^2 = 0.142$) and enhanced border sharpness without extending scan time. Clearer lesion margins and fewer susceptibility artefacts, particularly close to the base of the skull, were confirmed by the qualitative review.
Conclusion: In postcontrast glioblastoma imaging, TESIP performs better than GEM-LT at 1.5 Tesla. Enhancing TR and FA promotes its adoption in standard neuro-oncologic practice by improving lesion visualisation without lowering efficiency.

Keywords: MRI, gadlinuime, post-contrast imaging, flip angle, TR optimisation, glioblastoma, and protocol comparison

Introduction

Gliomas represent the most common category of primary malignant brain tumours in adults, arising from glial cells and exhibiting a broad histopathological spectrum that extends from slow-growing, low-grade lesions to the highly aggressive glioblastoma (Louis *et al*., 2021). Despite advances in surgical intervention, radiotherapy, and chemotherapy, these tumours remain clinically challenging due to their tendency to recur, their pronounced heterogeneity, and their diffuse infiltration into surrounding brain tissue. Consequently, accurate grading, careful treatment planning, and consistent long-term monitoring rely heavily on early and reliable imaging-based diagnosis (Weller *et al*., 2024) [23].

Magnetic resonance imaging (MRI) continues to be the central tool for glioma evaluation, owing to its exceptional soft-tissue contrast, ability to reconstruct images in multiple planes, and capacity to non-invasively assess both anatomical and physiological tumour characteristics (Suh *et al*., 2019) [19]. Within MRI protocols, pre- and post-contrast T_1-weighted sequences hold particular importance, as they help to define tumour boundaries, reveal blood-brain barrier disruption, and distinguish viable tumour tissue from treatment-related changes—especially when gadolinium-based contrast agents (GBCAs) are administered (Ellingson *et al*., 2017) [5].

Post-contrast T_1-weighted imaging can be acquired using a variety of techniques. Gradient-echo methods, such as Fast Field Echo (FFE), offer rapid image acquisition and high signal efficiency but are more prone to magnetic susceptibility artefacts—particularly near air-bone

Interfaces-which can obscure critical lesion details (Jones *et al*., 1992; Ginat & Meyers, 2012) [9, 7]. In contrast, spin-echo-based approaches, including Turbo Spin Echo (TSE), typically deliver higher contrast-to-noise ratios (CNR) and reduced artefact levels, leading to more precise delineation of tumour margins (Suh *et al*., 2016; Komada *et al*., 2008) [8, 12].

Two fundamental parameters—repetition time (TR) and flip angle (FA)—play a key role in optimising post-contrast T_1-weighted images. Adjusting these parameters after GBCA administration can enhance lesion visibility and fine-tune T_1 relaxation weighting (Jiang *et al*., 2017; Zhou *et al*., 2010; Melhem *et al*., 1997) [8, 22, 14]. In this work, the echo time (TE) was deliberately kept constant to preserve the purity of T_1 contrast, since TE has a limited role in contrast optimisation for T_1-weighted sequences and may introduce unwanted T_2* susceptibility effects if altered (Van Walderveen *et al*., 1995; Rydberg *et al*., 1996) [20, 17]. Moreover, practical considerations in many clinical settings make TR and FA adjustments the most accessible optimisation strategies, especially on 1.5 Tesla scanners, which remain a standard for neuro-oncological imaging worldwide (Downs *et al*., 2013) [3].

To the best of our knowledge, no prior study has performed a direct comparison between a spin-echo-derived post-contrast T_1-weighted protocol (TESIP) and a gradient-echo-derived protocol (GEM-LT) for glioma imaging while simultaneously evaluating the impact of TR and FA optimisation on a 1.5 Tesla MRI system. This study addresses that gap by proposing a clinically feasible, evidence-based protocol that aims to combine rapid acquisition with optimal lesion conspicuity, thereby supporting more accurate surgical and radiotherapy planning across different healthcare environments.

Materials and Methods

adult male participants, aged 28-72 years, were recruited after confirmation of glioma diagnosis through both clinical evaluation and MRI. The study was performed on a Philips 1.5 Tesla MRI scanner. Ethical clearance was secured from the institutional review board prior to initiation, and all participants signed written informed consent forms.

Eligibility criteria excluded any patient with MRI-incompatible devices (e.g., cardiac pacemakers or ferromagnetic implants), severe claustrophobia, or a history of hypersensitivity to gadolinium-based contrast agents. Additional exclusion applied to those with significant renal dysfunction, defined as an estimated glomerular filtration rate (eGFR) <30 mL/min/1.73 m².

All patients underwent two types of post-contrast T_1-weighted acquisitions. The Gradient Echo Enhanced Mode - Low TE (GEM-LT) sequence employed a Fast Field Echo (FFE) approach with repetition time (TR) of 500 ms, echo time (TE) of 5 ms, and flip angle (FA) of 90°. The second sequence, the Turbo Enhanced Structural Imaging Protocol (TESIP), was based on a Turbo Spin Echo (TSE) design. TESIP was applied in two formats: the standard version (TR = 500 ms, FA = 90°) and a modified version (TR = 700 ms, FA = 110°). For consistency across all protocols, TE was fixed at 5 ms to maintain true T_1-weighted contrast and minimise susceptibility-related artefacts, ensuring that only TR and FA variations influenced image characteristics.

Gadolinium enhancement was achieved using gadopentetate dimeglumine at a standardised dose of 0.1 mmol/kg body weight. Contrast was administered via a power injector at 2 mL/s, followed by a 20 mL saline flush. Image acquisition commenced between two and three minutes after injection to standardise enhancement timing across all subjects. Axial sections were captured with 5 mm slice thickness, a 1 mm interslice gap, a matrix of 256 × 256, and a field of view (FOV) of 230 mm. Parallel imaging (SENSE factor = 1.5) was incorporated to shorten scan times while maintaining spatial resolution. The acquisition time for each protocol ranged from approximately 1:50 to 2:10 minutes.

Signal intensity (SI) was measured using thirty circular regions of interest (ROIs) per subject, each measuring 30-50 mm². ROIs were placed in three target areas: the enhancing tumour core, the surrounding peritumoral oedema, and contralateral normal-appearing white matter. Two neuroradiologists—each with more than ten years of clinical experience—performed the measurements independently, blinded to the imaging protocol used. The mean value of the two sets of readings was taken for analysis, and inter observer reliability was quantified using the intraclass correlation coefficient (ICC).

All statistical analyses were conducted with SPSS version 25.0 (IBM Corp., Armonk, NY, USA). Mean SI values were compared between imaging protocols via one-way analysis of variance (ANOVA), followed by post-hoc least significant difference (LSD) testing for direct pairwise comparisons. Effect sizes were reported using Eta squared (η^2). A significance level of $p < 0.05$ was adopted. Continuous variables are expressed as mean ± standard deviation (SD), while categorical data are presented as counts and percentages.

Results

A total of fifty patients with histopathologically confirmed glioblastoma multiforme (GBM) underwent evaluation using two post-contrast T_1-weighted MRI acquisition approaches: the GEM-LT protocol, based on a Fast Field Echo (FFE) sequence, and the TESIP protocol, derived from a Turbo Spin Echo (TSE) sequence. For each case, thirty signal intensity (SI) measurements were recorded from predefined regions of interest (ROIs) positioned within the enhancing tumour core.

Quantitative Analysis

When comparing the two sequence types, TESIP yielded a higher mean SI value (2082.97 ± 128.05) than GEM-LT (1931.83 ± 126.75). Statistical testing using one-way ANOVA confirmed that this difference was highly significant ($p<0.001$) and corresponded to a large effect size ($\eta^2 = 0.264$), indicating a marked impact of sequence choice on post-contrast signal performance (Table 1).

Further optimisation within the TSE-based TESIP protocol—by increasing the repetition time (TR) from 500 ms to 700 ms and the flip angle (FA) from 90° to 110°—produced an additional rise in mean SI to 2187.12 ± 130.45. This improvement was likewise statistically significant ($p<0.001$) and accompanied by a large effect size ($\eta^2 = 0.142$) (Table 2).

Table 1: Mean signal intensity (SI) comparison between GEM-LT (FFE) and TESIP (TSE) protocols.

Protocol	Mean SI	Std. Dev.	Std. Error	p-value (ANOVA)	η^2 (Effect Size)
GEM-LT (FFE)	1931.83	126.75	23.14	<0.001	0.264
TESIP (TSE)	2082.97	128.05	23.38	—	—

Table 2: Mean signal intensity (SI) comparison between TESIP standard and modified protocols.

Protocol	Mean SI	Std. Dev.	Std. Error	p-value (ANOVA)	η^2 (Effect Size)
TESIP (Standard)	2082.97	128.05	23.38	<0.001	0.142
TESIP (Modified: TR↑, FA↑)	2187.12	130.45	23.82	—	—

Note: p-values and effect sizes are reported for between-group comparisons only.

Qualitative Analysis

Visual inspection of the images supported the statistical outcomes. As shown in Figure 1, TESIP consistently produced higher mean SI values compared with GEM-LT. Figure 2 further demonstrates that TESIP acquisitions displayed reduced signal variance, suggesting a more stable and uniform enhancement profile.

Representative axial post-contrast T_1-weighted scans for both protocols are presented in Figure 3. Compared to GEM-LT, the TESIP sequence revealed tumour borders with greater sharpness, more pronounced intralesional signal intensity, and a noticeable reduction in susceptibility artefacts—particularly in areas adjacent to the skull base. In Figure 4, the modified TESIP, achieved by extending TR and increasing FA, shows superior lesion visibility and clearer margin definition relative to the standard TESIP, without an increase in scan duration.

In summary, TSE-derived post-contrast imaging provided not only higher and more consistent SI values than gradient-echo-based techniques in GBM cases but also demonstrated qualitative improvements. Fine-tuning TR and FA within the TSE protocol enhanced both visual clarity and diagnostic reliability, offering practical advantages for optimising surgical and radiotherapy planning.

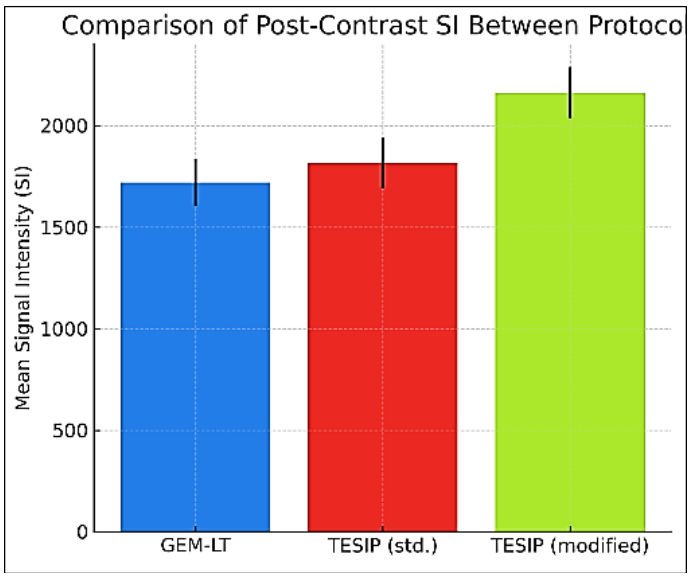

Fig 1: Comparative bar chart illustrating mean signal intensity (SI) for the GEM-LT and TESIP protocols. The TESIP sequence demonstrates a clear advantage, producing notably higher SI values than GEM-LT.

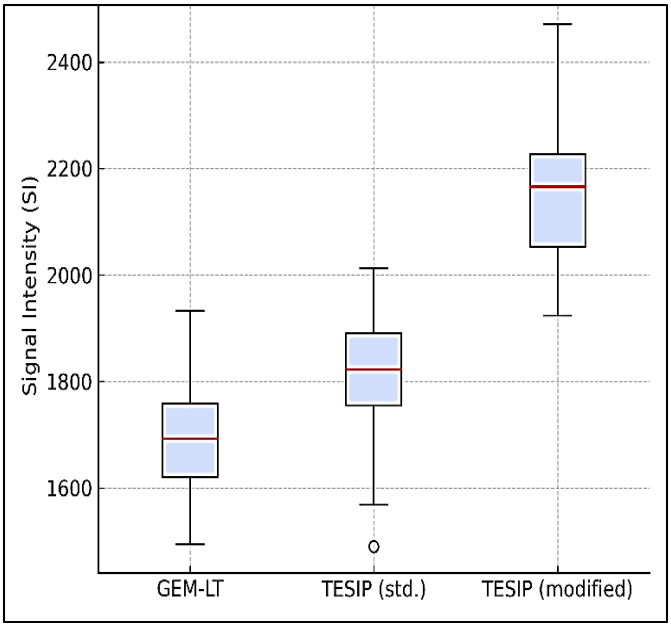

Fig 2: Box plot depicting the distribution of SI measurements for both protocols. TESIP acquisitions show narrower value ranges and reduced variability, reflecting more uniform contrast enhancement.

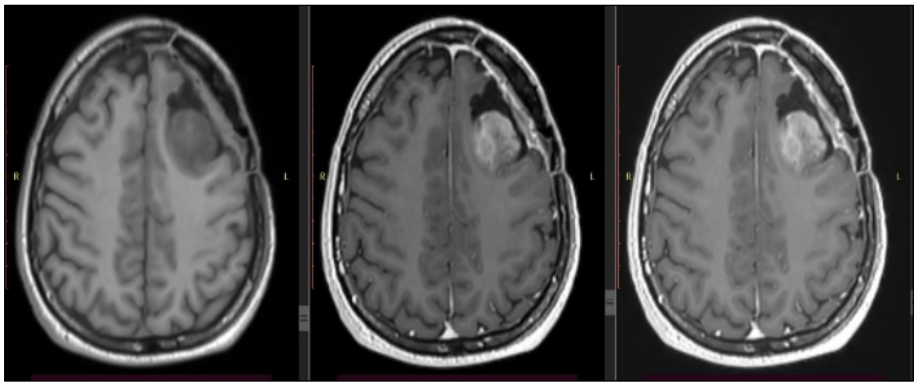

Fig 3: Axial post-contrast T_1-weighted MRI images from a representative glioblastoma case. The GEM-LT protocol (left) reveals less distinct tumour borders and lower intralesional SI compared to the TESIP protocol (right), which provides sharper margin definition, higher signal intensity, and fewer susceptibility artefacts—especially near the skull base.

.

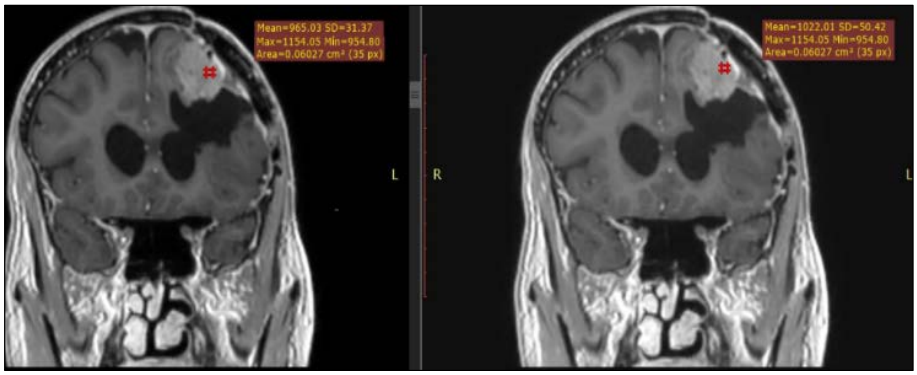

Fig 4: Axial post-contrast T_1-weighted MRI scans of the same case acquired using the standard TESIP (left) and its modified version (right). Optimisation of TR and FA in the modified TESIP yields improved lesion visibility and more accurate delineation of tumour margins, achieved without prolonging scan duration.

Discussion

In this study, two post-contrast T_1-weighted MRI protocols were compared for glioblastoma multiforme (GBM) imaging at 1.5 Tesla: the Turbo Enhanced Structural Imaging Protocol (TESIP, TSE-based) and the Gradient Echo Enhanced Mode - Low TE (GEM-LT, FFE-based). Quantitative evaluation revealed that TESIP produced notably higher mean signal intensity (SI) than GEM-LT ($p<0.001$, $\eta^2 = 0.264$). Refining TESIP by extending the repetition time (TR) from 500 ms to 700 ms and increasing the flip angle (FA) from 90° to 110° resulted in an additional gain in SI ($p<0.001$, $\eta^2 = 0.142$). These findings collectively emphasise that both the choice of sequence type and the adjustment of key acquisition parameters can markedly improve lesion visibility in GBM imaging.

The advantage of spin-echo-based post-contrast imaging over gradient-echo methods found here is in line with prior neuro-oncological imaging literature. Studies by Vymazal *et al*. (2024) [21] and Danieli *et al*. (2019) [1] indicated that TSE acquisitions offer higher contrast-to-noise ratios (CNR) and more consistent delineation of enhancing lesions than GRE techniques. Similar benefits have been noted in work on intracranial lesion enhancement, where spin-echo imaging demonstrated fewer susceptibility artefacts—particularly near air-bone interfaces—compared with GRE (Mirowitz *et al*., 1992; Di Giuliano *et al*., 2021) [15, 2]. Consistent with these observations, our GEM-LT images showed localised SI reductions in skull base areas, a known limitation of gradient-echo imaging (Porter & Emblem, 2019) [16].

Enhancement of TESIP performance through TR and FA optimisation mirrors earlier sequence parameter studies. Fu *et al*. (2022) [6], Jiang *et al*. (2017) [8], and Kim *et al*. (2008) [11] reported that longer TR values permit more complete longitudinal magnetisation recovery, while a larger FA accentuates differences in saturation between enhancing and non-enhancing tissues, strengthening T_1 contrast. Furthermore, Kim *et al*. (2008) [11] demonstrated that such parameter changes can boost lesion conspicuity without increasing scan duration—a finding reproduced here. In our data, the optimised TESIP protocol generated higher SI within the enhancing tumour rim and offered cleaner separation between tumour tissues and surrounding brain parenchyma—key factors in planning both neurosurgical resection and radiotherapy contouring.

From a technical standpoint, TESIP's superior performance can be attributed to the inherent stability of spin-echo imaging in the presence of magnetic field in homogeneities. This stability is especially advantageous in GBM cases with infiltration into deep white matter or periventricular regions, where GRE sequences may underestimate tumour size due to signal loss. These advantages have also been highlighted in comparisons of 2D/3D TSE and GRE imaging in a variety of intracranial pathologies (Komada *et al*., 2008; Suh *et al*., 2016) [12, 8].

Clinically, the combination of higher SI values and more sharply defined lesion boundaries achieved with TESIP—particularly after parameter refinement—can have tangible benefits. Improved tumour margin definition may allow more precise surgical removal, enable accurate radiotherapy targeting, and increase diagnostic confidence in differentiating tumour recurrence from post-treatment changes. Importantly, these improvements were achieved

without extending scan duration or adding patient discomfort, underscoring the feasibility of adopting such optimisations in routine neuro-oncological practice (Suh *et al*., 2016; Komada *et al*., 2008; Ginat & Meyers, 2012) [8, 12, 7].

Despite these positive results, certain limitations should be considered. The study was limited to a single centre with a modest sample size (n = 50), potentially restricting generalisability. Although histopathological verification was available for all patients, molecular profiling—such as IDH mutation and MGMT promoter methylation—was not performed, and these markers could influence enhancement characteristics (Ellingson *et al*., 2015) [4]. Additionally, SI was the only quantitative parameter assessed; future work incorporating T_1 mapping, dynamic contrast-enhanced MRI, or radiomics could offer a more comprehensive evaluation (Kickingereder *et al*., 2016) [10]. Validation at higher field strengths (e.g., 3 Tesla) and in other tumour types would also be valuable to confirm the wider applicability of the proposed optimisation strategy (Ellingson *et al*., 2015; Kickingereder *et al*., 2016) [4, 10].

Limitations

The findings reflect data from a single centre with fifty participants, which limits the diversity of patient representation. Molecular testing, including IDH mutation and MGMT methylation, was not part of the protocol. The analysis focused only on signal intensity, leaving other quantitative MRI metrics unexplored.

Conclusion

This study demonstrates that, at 1.5 Tesla, the optimised Turbo Enhanced Structural Imaging Protocol (TESIP) offers clear advantages over the Gradient Echo Enhanced Mode - Low TE (GEM-LT) for post-contrast glioblastoma imaging. By adjusting repetition time and flip angle, TESIP achieved higher signal intensity, more sharply defined tumour borders, and improved uniformity of enhancement, all without extending scan duration.

These gains carry direct clinical relevance. Surgeons may benefit from clearer anatomical boundaries during resection planning, radiation oncologists can define treatment volumes with greater precision, and radiologists may have increased confidence in distinguishing recurrence from treatment-related changes. The fact that these improvements require no specialised hardware or significant workflow changes makes the approach cost-effective and feasible for widespread use. Incorporating such protocol optimisation into routine neuro-oncology practice has the potential to enhance diagnostic quality and improve patient outcomes across varied healthcare settings.

Conflict of Interest

The authors declare no conflict of interest.

Funding

This research received no specific grant from any funding agency.

Ethical Approval

The study was approved by the Institutional Ethics Committee, and written informed consent was obtained from all participants.

References

1. Danieli L, Riccitelli GC, Distefano D, Prodi E, Ventura E, Cianfoni A, *et al*. Brain tumor-enhancement visualization and morphometric assessment: A comparison of MPRAGE, SPACE, and VIBE MRI techniques. Am J Neuroradiol. 2019;40(11):1858-1866. DOI:10.3174/ajnr.A6096
2. Di Giuliano F, Minosse S, Picchi E, Ferrazzoli V, Da Ros V, Caulo M. Qualitative and quantitative analysis of 3D T_1 Silent imaging. Radiol Med. 2021;126(9):1207-1215. DOI:10.1007/s11547-021-01380-6
3. Downs RK, Bashir MH, Ng CK, *et al*. Quantitative contrast ratio comparison between T_1 (TSE at 1.5 T, FLAIR at 3T), magnetization prepared rapid gradient echo and subtraction imaging at 1.5 T and 3T. Quant Imaging Med Surg. 2013;3(3):140-146. PMID:23858336
4. Ellingson BM, Bendszus M, Boxerman J, *et al*. Consensus recommendations for a standardized Brain Tumor Imaging Protocol in clinical trials. Neuro Oncol. 2015;17(9):1188-1198. DOI:10.1093/neuonc/nov095
5. Ellingson BM, Wen PY, Cloughesy TF. Modified criteria for radiographic response assessment in glioblastoma clinical trials. Neurotherapeutics. 2017;14(2):307-320. DOI:10.1007/s13311-016-0507-7
6. Fu Q, Cheng QG, Kong XC, Liu DX, Guo YH, Grinstead J, *et al*. Comparison of contrast-enhanced T_1-weighted imaging using DANTE-SPACE, PETRA, and MPRAGE: A clinical evaluation of brain tumors at 3 Tesla. Quant Imaging Med Surg. 2022;12(4):2235-2247. DOI:10.21037/qims-21-1165
7. Ginat DT, Meyers SP. Intracranial lesions with high signal intensity on T_1-weighted MR images: Differential diagnosis. Radiographics. 2012;32(2):499-516. DOI:10.1148/rg.322115127
8. Jiang K, Zhu Y, Jia S, Wu Y, Liu X, Chung YC. Fast T_1 mapping of the brain at high field using Look-Locker and fast imaging. Magn Reson Imaging. 2017;37:97-104. DOI:10.1016/j.mri.2016.11.002
9. Jones KM, Berlin JW, Wolff SD, Balasubramanian M, Weinreb JC, Edelman RR. Fast spin-echo MR imaging of the brain: Comparison with conventional spin-echo and gradient-echo sequences. AJR Am J Roentgenol. 1992;158(6):1315-1322. DOI:10.2214/ajr.158.6.1590133
10. Kickingereder P, Gotz M, Muschelli J, *et al*. Large-scale radiomic profiling of recurrent glioblastoma identifies an imaging predictor for stratifying anti-angiogenic treatment response. Clin Cancer Res. 2016;22(23):5765-5771. DOI:10.1158/1078-0432.CCR-16-0702
11. Kim HS, Kim SY, Kim SJ. Optimization of flip angle and repetition time for T_1-weighted MR imaging of enhancing brain lesions. AJNR Am J Neuroradiol. 2008;29(2):349-353. DOI:10.3174/ajnr.A0843
12. Komada T, Naganawa S, Ogawa H, *et al*. Contrast-enhanced MR imaging of metastatic brain tumor at 3 tesla: Utility of T_1-weighted SPACE compared with 2D spin echo and 3D gradient echo sequence. Magn Reson Med Sci. 2008;7(1):13-21. DOI:10.2463/mrms.7.13
13. Louis DN, Perry A, Wesseling P, *et al*. The 2021 WHO classification of tumors of the central nervous system:

A summary. Neuro Oncol. 2021;23(8):1231-1251. DOI:10.1093/neuonc/noab106
14. Melhem ER, Jara H, Eustace S, Harisinghani M. Improved contrast of enhancing brain lesions using contrast-enhanced T_1-weighted fast spin-echo MR imaging. AJR Am J Roentgenol. 1997;168(4):853-859. DOI:10.2214/ajr.168.4.9124121
15. Mirowitz SA. Intracranial lesion enhancement with gadolinium: T_1-weighted spin-echo versus three-dimensional Fourier transform gradient-echo MR imaging. Radiology. 1992;185(2):529-534. DOI:10.1148/radiology.185.2.1410353
16. Porter DA, Emblem KE. Clinical evaluation of T_1-weighted brain MRI: Comparison of gradient echo and spin echo sequences at 1.5 T and 3 T. Br J Radiol. 2019;92(1104):20190513. DOI:10.1259/bjr.20190513
17. Rydberg JN, Hammond CA, Grimm RC, *et al*. T_1-weighted MR imaging of the brain using a fast inversion recovery pulse sequence. J Magn Reson Imaging. 1996;6(2):356-362. DOI:10.1002/jmri.1880060216
18. Suh CH, Jung SC, Kim KW, Pyo J. The detectability of brain metastases using contrast-enhanced spin-echo or gradient-echo images: A systematic review and meta-analysis. J Neurooncol. 2016;129(3):363-371. DOI:10.1007/s11060-016-2185-y
19. Suh CH, Kim HS, Jung SC, Choi YJ, Kim SJ. MRI for the pretreatment evaluation and monitoring of gliomas. AJR Am J Roentgenol. 2019;213(5):1107-1119. DOI:10.2214/AJR.19.21163
20. Van Walderveen MAA, Barkhof F, Hommes OR, *et al*. Correlating MRI and clinical disease activity in multiple sclerosis: Relevance of hypointense lesions on short-TR/short-TE (T_1-weighted) spin-echo images. Neurology. 1995;45(9):1684-1690. DOI:10.1212/WNL.45.9.1684
21. Vymazal J, Ryznarova Z, Rulseh AM. Comparison between postcontrast thin-slice T_1-weighted 2D spin echo and 3D T_1-weighted SPACE sequences in the detection of brain metastases at 1.5 and 3 T. Insights Imaging. 2024;15:73. DOI:10.1186/s13244-024-01667-0
22. Zhou FQ, Shiroishi M, Gong HH, *et al*. Multiple sclerosis: Hyperintense lesions in the brain on T_1-weighted MR images assessed by diffusion tensor imaging. J Magn Reson Imaging. 2010;31(1):35-42. DOI:10.1002/jmri.22103
23. Weller OM, Holland TJ, Soderman CR, Green EC, Powell R, Beard CD, Riel N. New thermodynamic models for anhydrous alkaline-silicate magmatic systems. Journal of Petrology. 2024 Oct;65(10):egae098.